2D Ray-Tracing Simulation Software Customized for Studying Various Reconfigurable Intelligent Surface Optimization Problems

Jeong Min Kong[1], Jiguang He[2], George Alexandropoulos[2,3], and Merouane Debbah[2]

[1]Edward S. Rogers Sr. Department of Electrical and Computer Engineering, University of Toronto, Toronto, Canada
[2]AI and Digital Science Research Center, Technology Innovation Institute, Abu Dhabi, UAE
[3]Department of Informatics and Telecommunications, University of Athens, Athens, Greece

November 2022

1 Preliminaries

This section discusses about the background materials that are required to understand how the simulator was implemented.

1.1 Reflection and Transmission Angles

When an electromagnetic wave interacts with a medium that has a different refractive index than the one it travelled in, two waves are *usually* produced: reflected wave and transmitted wave.

The angle of the incident wave, reflected wave, and transmitted wave are all defined relative to a line normal to the interface between two mediums, as shown in Figure 1.

The angle of the reflected wave is the same as the angle of the incident wave, ie.

$$\theta_i = \theta_r \tag{1}$$

The angle of the transmitted wave follows the famous **Snell's Law**, ie.

$$\sin\theta_i = \sin\theta_t \tag{2}$$

Recall from earlier, that two waves are *usually* produced, but not always. In the case of **total internal reflection**, only reflected wave is produced. Total internal reflection is a special case of internal reflection, which is a term to describe reflection phenomena when the refractive index of the incident medium, n_i, is greater than or equal to the refractive index of the transmitted medium, n_t. Total internal reflection occurs when $n_i \geq n_t$, and:

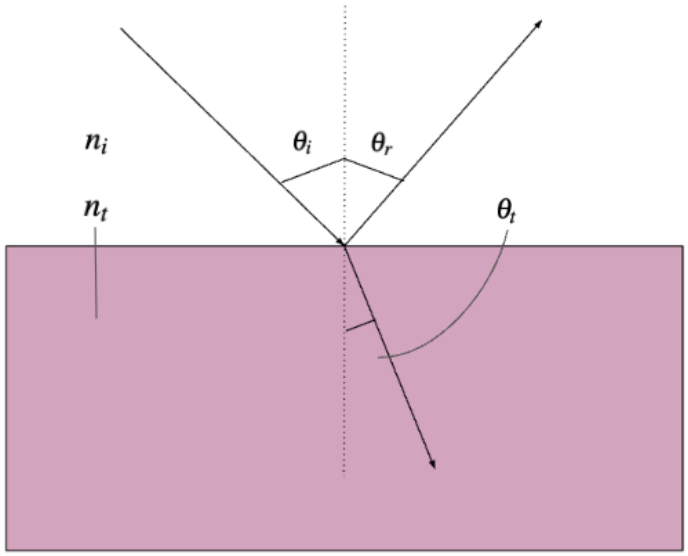

Figure 1: Incident wave, reflected wave, and transmitted wave at the interface.

$$\theta_i > \theta_c, \tag{3}$$
$$\theta_c = \arcsin \frac{n_t}{n_i}$$

1.2 Reflection and Transmission Coefficients

Electromagnetic wave will have one of the following two polarizations as it is hitting the interface: Transverse Electric (TE) or Transverse Magnetic (TM). The difference between these two polarizations is that TE waves' electric fields are perpendicular to the interface, whereas TM waves' electric fields are parallel to the interface. Since electric fields and magnetic fields are always orthogonal, this statement is equivalent to saying TE waves' magnetic fields are parallel to the interface, whereas TM waves' magnetic fields are perpendicular to the interface. For the simulator, we assume that all electromagnetic waves are TE.

Reflection coefficient and **transmission coefficient** are the most important values for describing an interface. Reflection coefficient indicates how much of the incident electric field is reflected, and transmission coefficient indicates how much of the incident electric field is transmitted. The reflection and transmission coefficients for TE waves are the following:

$$r = \frac{E_r}{E_i} = \frac{n_i \cos\theta_i - n_t \cos\theta_t}{n_i \cos\theta_i + n_t \cos\theta_t} \tag{4}$$

$$t = \frac{E_t}{E_i} = \frac{2n_i \cos\theta_i}{n_i \cos\theta_i + n_t \cos\theta_t} \tag{5}$$

1.3 Reflectance and Transmittance

Reflectance indicates how much of the incident wave's power is reflected, and **transmittance** indicates how much of the incident wave's power is transmitted. The reflectance and transmittance for TE waves are the following:

$$R = \frac{P_r}{P_i} = r^2 \tag{6}$$

$$T = \frac{P_t}{P_i} = \frac{n_t \cos\theta_t}{n_i \cos\theta_i} t^2 \tag{7}$$

Rearranging (6) and (7), we see that:

$$P_r = P_i R \tag{8}$$

$$P_t = P_i T \tag{9}$$

Note that $R + T = 1$. This implies that $P_i R + P_i R = P_i$, and with (8) and (9), $P_r + P_t = P_i$.

1.4 Fundamental Concepts in Wireless Communication

Free-Space Path Loss (FSPL):

$$FSPL = \frac{P_{source}}{P_{received}} = (\frac{4df\pi}{c})^2 \tag{10}$$

Noise:

$$Noise = 0.001(10^{\frac{\log(Bandwidth)-174}{10}}) \tag{11}$$

Signal-to-Noise Ratio (SNR):

$$SNR = \frac{\sum P_{desired}}{Noise} \tag{12}$$

Signal-to-Noise-Plus-Interference Ratio (SINR):

$$SINR = \frac{\sum P_{desired}}{Noise + \sum P_{interference}} \tag{13}$$

2 Simulation Input Parameters

Important information that users will indicate prior to running the simulation:

1) Dimensions and refractive index of the environment

2) Information about the rectangular objects in the environment:

- Low and high x-bounds of the rectangular object
- Low and high y-bounds of the rectangular object
- Refractive index of the rectangular object

3) Information about the reconfigurable intelligent surfaces (RISs) in the environment:

- ID of the rectangular object that the RIS is placed on
- Which of the four sides of the rectangular object the RIS is placed on
- Low and high bounds of the RIS
- Time frames for which the RIS is active
- Beamforming direction of the RIS, measured counter-clockwise from the RIS, during each time frame
- Reflectance of the RIS during each time frame

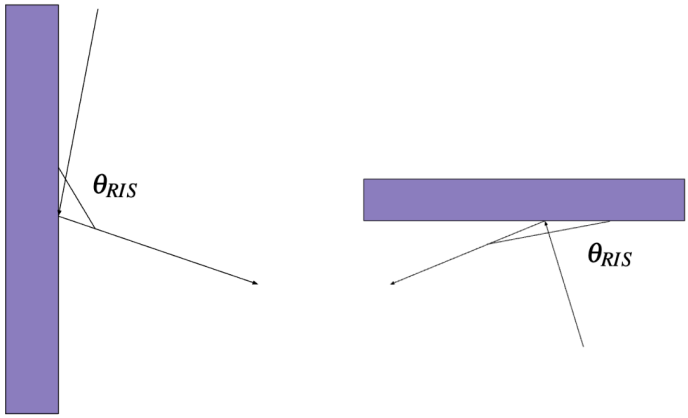

Figure 2: Examples illustrating how θ_{RIS} is measured.

4) Information about the source rays in the environment:

- Position of the ray
- Direction of the ray with respect to the +ve x-axis
- Power of the ray
- Frequency of the ray
- Transmission time of the ray

5) Information about the receivers in the environment:

- Position of the receiver
- Radius of the receiver
- Ray IDs the receiver considers desired

3 Key Methods

3.1 Finding the Intersection Point of the Ray

Step 1:

We express the ray as a linear function, $f_{ray}(x) = \nabla f_{ray}(x)x + y_{intercept}$. We find this expression by:
1) computing $\nabla f_{ray}(x) = \frac{\sin\theta_{dir}}{\cos\theta_{dir}}$, where θ_{dir} is the direction of the ray with respect to the +ve x-axis.
2) computing $y_{intercept} = y_{pos} - \nabla f_{ray}(x)$, where y_{pos} is the y-position of the ray.

Step 2:

We make an assumption that each dimension of every object is infinitely long, and find the intersection point between each of these and f_{ray}. Of course, the intersection point between a vertical dimension and f_{ray} is just $(x^{'}, f_{ray}(x^{'}))$, where $x^{'}$ is the x-value of the vertical dimension. The intersection point between a horizontal dimension and f_{ray} is $(\frac{y^{'} - y_{intercept}}{\nabla f_{ray}}, y^{'})$, where $y^{'}$ us the y-value of the horizontal dimension.

Step 3:

For each intersection point computed in step 2), we check whether it is within the bounds of the corresponding dimension; if it is not within the bounds, we don't consider it in the subsequent steps. Let's say we are considering the object from Figure 3 as an example. If the intersection point between infinitely-long dimension 1 and f_{ray} does not lie between y = 5 and y = 15, then we immediately know that the ray will not intersect with this dimension.

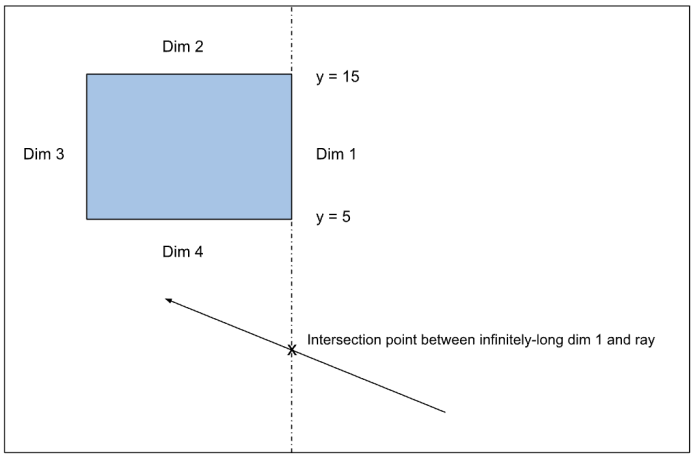

Figure 3: Example scenario with one object in the environment.

Step 4:

In step 3), we reduced the number of intersection point candidates. We make further progress in this step by now considering the direction of the ray. Let's consider the scenario in Figure 4 as an example. Here, because the ray's direction is in 2nd quadrant, we immediately know that it will not intersect with object 2 and 3; therefore, in subsequent steps, we don't consider the intersection points between f_{ray} and dimensions of object 2 and 3. We use this reasoning for all ray directions.

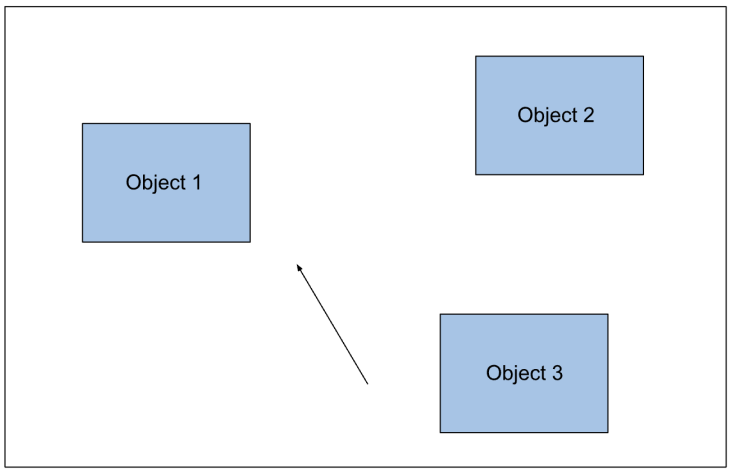

Figure 4: Example scenario with multiple objects in the environment.

Step 5:

In this final step, we measure the distance between the position of the ray and every remaining intersection point candidates. The intersection point candidate that yields the smallest distance is indeed the interface point that the ray will hit.

3.2 Determining the Properties of Reflection and Transmission Rays

This subsection discusses how we determine some of the important properties of newly-created reflection and transmission rays, namely: initial power of the rays, initial position of the rays, and direction of the rays with respect to the x-axis.

Initial Power

The initial power of reflection ray is determined using (8). P_i is the power its parent ray had before colliding with the interface, and this can be computed using the path loss formula from (10), together with parent ray's initial power, frequency, and distance travelled. R is equal to 1 if condition (3) is satisfied (ie. there is total internal reflection). If the point on the interface that its parent ray hit lies within an RIS that is active, then R is the reflectance of the RIS. Otherwise, R is found using (6).

The initial power of transmission ray is determined using (9). P_i can be computed in the same way as above. T is equal to 0 if condition (3) is satisfied, and/or if the point on the interface that its parent ray hit lies within an RIS that is active; otherwise, T is found using (7).

Initial Position

The initial position of both reflection and transmission rays is the point on the interface that its parent ray hit. This can be easily seen from Figure 1.

Direction

There are three scenarios to consider:

Scenario 1 - There is no RIS on the interface or total internal reflection.

In this scenario, when the parent ray hits the interface, both reflection and transmission rays are created. Of course, as discussed in the preliminaries section, the reflection and transmission angles with respect to the line normal to the interface always follows (1) and (2), respectively. However, as specified in earlier sections, the direction of the rays are measured with respect to the +ve x-axis. We have to therefore consider various cases and apply appropriate transformations to find rays' directions in accordance to this definition. See Table 1 below.

Case	Reflection Angle wrt +ve x-axis	Transmission Angle wrt +ve x-axis
Parent Ray Intersected: Vertical Interface (x-bound). Parent Ray Direction: Quadrant 1	$\pi - \theta_r$	θ_t
Parent Ray Intersected: Vertical Interface (x-bound). Parent Ray Direction: Quadrant 2	θ_r	$\pi - \theta_t$
Parent Ray Intersected: Vertical Interface (x-bound). Parent Ray Direction: Quadrant 3	$2\pi - \theta_r$	$\pi + \theta_t$
Parent Ray Intersected: Vertical Interface (x-bound). Parent Ray Direction: Quadrant 4	$\pi + \theta_r$	$2\pi - \theta_t$
Parent Ray Intersected: Horiz. Interface (y-bound). Parent Ray Direction: Quadrant 1	$\frac{3\pi}{2} + \theta_r$	$\frac{\pi}{2} - \theta_t$
Parent Ray Intersected: Horiz. Interface (y-bound). Parent Ray Direction: Quadrant 2	$\frac{3\pi}{2} - \theta_r$	$\frac{\pi}{2} + \theta_t$
Parent Ray Intersected: Horiz. Interface (y-bound). Parent Ray Direction: Quadrant 3	$\frac{\pi}{2} + \theta_r$	$\frac{3\pi}{2} - \theta_t$
Parent Ray Intersected: Horiz. Interface (y-bound). Parent Ray Direction: Quadrant 4	$\frac{\pi}{2} - \theta_r$	$\frac{3\pi}{2} + \theta_t$

Table 1. Reflection and transmission angles with respect to +ve x-axis for different cases. θ_r is the reflection angle with respect to the line normal to the interface, and θ_t is the transmission angle with respect to the line normal to the interface.

Scenario 2 - There is RIS on the interface.

In this scenario, just reflection ray is created.

There are two possible directions that the reflection ray can take. If the parent ray's intersection point on the interface does not lie within the bounds of the RIS, and/or if the parent ray's intersection time does not

lie within the time frame for which the RIS is active, then the reflection ray's direction with respect to the +ve x-axis can be determined using Table 1. However, if the parent ray's intersection point lies within the bounds of the RIS, and the intersection time lies within the time frame for which the RIS is active, then the reflection ray is going to be directed in the beamforming angle set by the RIS in that time frame. Note: as specified in the simulation input parameters section and shown in Figure 2, the beamforming angle set by the RIS is measured counter-clockwise from the RIS; therefore, similar to the previous scenario, we have to apply appropriate transformation to the beamforming angle set by the RIS to derive the reflection angle with respect to the +ve x-axis. See Table 2 below.

Case	Reflection Angle wrt +ve x-axis
RIS Orientation: Vertical (x-bound). Responds to: Rays from Left	$\frac{3\pi}{2} - \theta_{RIS}$
RIS Orientation: Vertical (x-bound). Responds to: Rays from Right	$\frac{\pi}{2} - \theta_{RIS}$
RIS Orientation: Horizon. (y-bound). Responds to: Rays from Below	$2\pi - \theta_{RIS}$
RIS Orientation: Horizon. (y-bound). Responds to: Rays from Top	$\pi - \theta_{RIS}$

Table 2. Reflection angle with respect to +ve x-axis for different cases involving RIS. θ_{RIS} is the beamforming angle set by the RIS, measured counter-clockwise from the RIS.

Scenario 3 - There is total internal reflection.

As discussed in the preliminaries section, when there is total internal reflection, just reflection ray is created. The direction of the reflection ray, with respect to the +ve x-axis, can be found using Table 1.

3.3 Computing SNR and SINR at the Receiver

SNR:

At any given time during the simulation run, when a ray, which is travelling at a speed of $\frac{c}{n}$, is within the radius of the receiver, the power of the ray is added to the receiver. Using this cumulative power value at the receiver, SNR is computed real-time using (12).

SINR:

In this simulator, every source ray is given a unique ID, and all of the rays in its "bloodline" inherit this ID. For example, if the ID of the source ray is 0, its reflection and transmission rays also have ID of 0, the reflection and transmission rays of these rays also have ID of 0, and so on.

As noted in the simulation input parameters section, each receiver has a list of ray IDs that it considers as "desired". Similar to SNR, at any given time during the simulation run, when a ray's location is within the radius of the receiver, the ray is captured by the receiver. However, unlike SNR, we evaluate whether this

captured ray is considered desired or interference, by checking if its ID matches with any ID in the receiver's list. If there is a match, the power of this captured ray is added to the desired power variable of the receiver; if there is no match, the power of this captured ray is added to the interference power variable of the receiver. Let's look at the example illustrated in Figure 5. Because the desired ray IDs for the receiver are 0 and 2, the powers from the rays with ID 0 and 2 are considered desired, whereas the power from the ray with ID 1 is considered interference. Using these cumulative desired and interference power values at the receiver, SINR is computed real-time using (13).

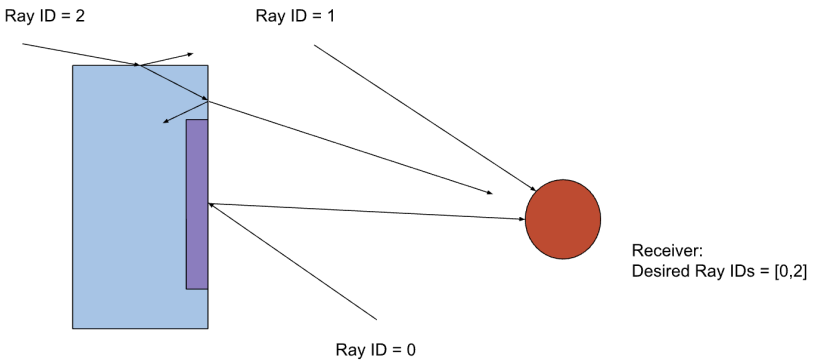

Figure 5: Example illustrating which rays the receiver considers as desired and which as interference.

4 Results

With the simulator, it is possible to: 1) track the SINRs of the receivers and the positions of the rays at every time-increment of the simulation run, and 2) obtain the SINR heatmap at the final time of the simulation run. Let's consider a simple-example shown in Figure 6 to better understand these functionalities.

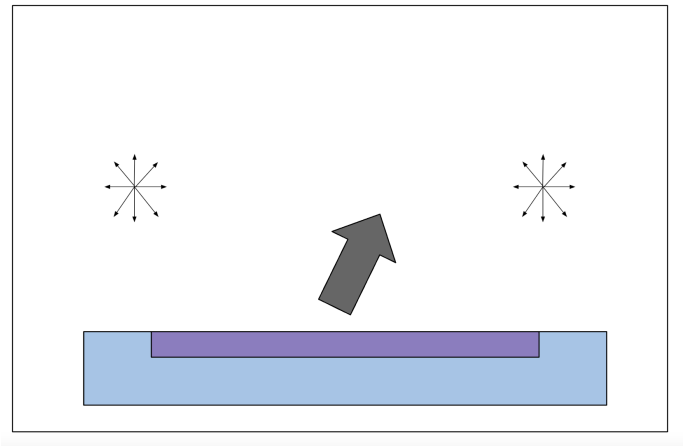

Figure 6: Example simulation set-up. Thin arrows represent omnidirectional sources, blue rectangle represents an object, purple rectangle represents an RIS, and thick arrow represents the beamforming direction of the RIS, which is 0.55π here (counter-clockwise from the RIS).

If the user specifies receiver locations as shown in Figure 7 a), and decides to use functionality 1), the

simulator will output results like the ones shown in Figure 7 b) and c). The user can see the positions of all the rays at different times, and also see the SINR values at all the receivers at different times through the terminal.

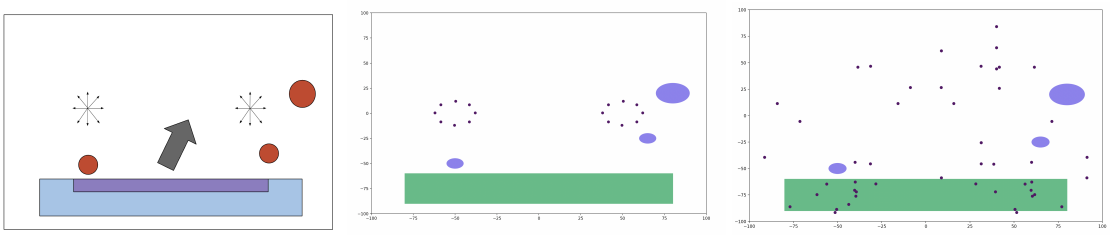

Figure 7: a) Same simulation set-up as Figure 6. Red are the receivers. b) Plot showing the positions of the rays at t = 1×10^{-8} s. c) Plot showing the positions of the rays at t = 5×10^{-8} s.

If the user decides to use functionality 2), the simulator will output Figure 8 a). This plot shows what SINR would be if a receiver was placed at each incremental location in the environment.

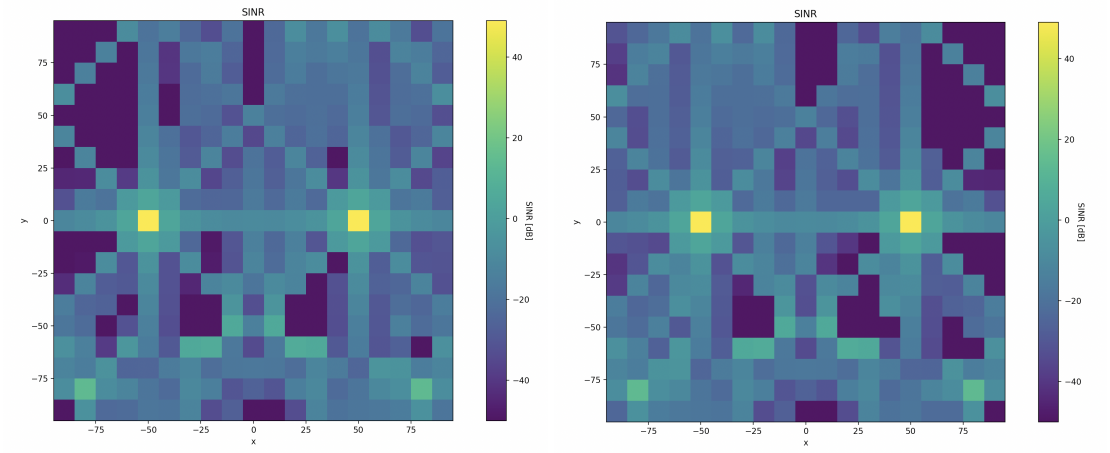

Figure 8: a) SINR heatmap of the simulation set-up from Figure 6. b) SINR heatmap of the simulation set-up from Figure 6, except $\theta_{RIS} = 0.45\pi$ instead of $\theta_{RIS} = 0.55\pi$. This is to just briefly illustrate how much impact RIS's beamforming direction can have on different regions' wireless coverage.

We have started developing several tools that would allow the user to quickly attain a large set of performance data, such as wireless coverage, for various parameter values. For example, Figure 9 shows the SINR outage probabilities when the RIS from the simulation set-up in Figure 6 have different beamforming angle values, ranging from 0° to 180°.

5 Future Work

There are several updates we would like to make to the simulator in the future.

1) The simulator currently only considers reflection and transmission (also known as refraction); however, we would also like to consider scattering in the future.

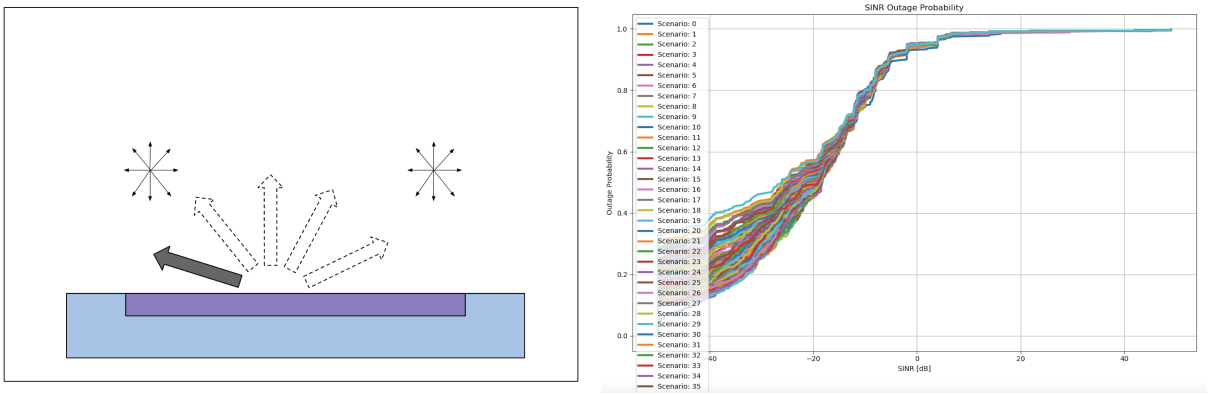

Figure 9: SINR outage probabilities for different RIS beamforming angles.

2) We would like to make it possible to measure delay spread at the receivers.
3) The simulator currently assumes that RISs only have reflecting abilities. However, recent literature [3] have proposed a new model of RISs called Simultaneously Transmitting and Reflecting RISs (also known as STAR-RISs), which, like the name suggests, have the ability to both transmit and reflect rays. We would like to also incorporate these to the simulator in the future.

More immediately, we will use this simulator to gather a large collection of data & approach various RIS optimization problems with machine learning. We will also use this simulator as an experimental tool to examine the validity of many theoretical results from RIS papers published over the past few years.

6 References

[1] F. L. Pedrotti, L. M. Pedrotti, and L. S. Pedrotti, Introduction to Optics, 3rd ed. Cambridge: Cambridge University Press, 2017.

[2] D. Tse and P. Viswanath, Fundamentals of Wireless Communication. Cambridge, U.K.: Cambridge Univ. Press, 2005.

[3] Y. Liu, X. Mu, J. Xu, R. Schober, Y. Hao, H. V. Poor, and L. Hanzo, "STAR: Simultaneous transmission and reflection for 360 coverage by intelligent surfaces," IEEE Wireless Commun., vol. 28, no. 6, pp. 102–109, Dec. 2021.